Heat transfer simulation of the cure of thermoplastic particle interleaf carbon fibre epoxy prepregs

Tassos Mesogitis[a*], *James Kratz*[a], *Alex A Skordos*[b]

[a] *Advanced Composite Centre for Innovation and Science (ACCIS),*

University of Bristol, Queen's Building, University Walk, Bristol BS8 1TR, UK

[b] *School of Aerospace, Transport and Manufacturing,*

Cranfield University, Cranfield, United Kingdom, MK43 0AL

*corresponding author's email: t.mesogitis@bristol.ac.uk

Abstract

Thermochemical properties are needed to develop process models and define suitable cure cycles to convert thermosetting polymers into rigid glassy materials. Uncertainty surrounding the suitability of thermal analysis techniques and semi-empirical models developed for conventional composite materials has been raised for the new class of particle interleaf materials. This paper describes kinetics, conductivity, heat capacity, and glass transition temperature measurements of HexPly® M21 particle interleaf material. Thermal models describing conventional, non-particle epoxy systems were fit to the data and validated through a thick-section cure. Results from curing experiments agree with heat transfer simulation predictions, indicating that established thermal analysis techniques and models can describe polymerisation and evolving material properties during processing of a material representing the class of interleaf toughened systems. A sensitivity study showed time savings up to about 20%, and associated energy-efficiency-productivity benefits, can be achieved by using cure simulation for particle interleaf materials.

1. Introduction

A new class of interleaf toughened composite materials have found widespread application in recent high-performance aerospace applications because of superior damage tolerance [1-3]. The characteristic thick resin layer found in-between plies of interleaf composites creates a plastic zone ahead of any crack tips to improve delamination resistance [4-5]. The improved damage tolerance offered by interleaf composites could be compromised though cure induced defects, such as excessive temperature and degree-of-cure gradients that lead to a heightened residual stress state in the final composite material [6]. Cure simulation can minimise the effects of temperature processing history and optimise curing conditions to minimise internal stress build-up if appropriate thermal material models are available [7].

A significant body of work has focused on the development of experimental techniques and thermal models describing the kinetics of cure reaction processes, and evolving material properties relevant to energy transfer and absorption during cure of thermosetting polymers; some examples include [8-10]. Un-toughened polymers or reaction-induced phase separating materials form the basis of study for cure evolution influence on material properties. Important observations include how changes in physical properties, such as timing of vitrification in the temperature cycle can have a strong effect on the thermoplastic morphology in phase-separating polymers [11-12].

Particle interleaf composites tend to have a higher thermoplastic content than conventional non-particle toughened phase-separating systems in order to create the polymer rich interleaf. Conflicting views regarding the use of differential scanning calorimetry (DSC) to describe cure reactions of this class of material have been reported in the literature [13-17]. DSC is often used to measure the curing kinetics and degree-of-cure of polymer materials by relating the heat flow during elevated temperature processing to the fractional conversion. If DSC is

unable to describe the curing process of particle interleaf materials, new characterisation methods would be required for process cycle development.

This work explores material characterisation methods and modelling techniques of the thermochemical properties of particle interleaf carbon fibre epoxy prepregs. The cure kinetics, glass transition temperature, specific heat capacity, and thermal conductivity were measured through processing, using techniques developed for non-particle thermosetting materials. A series of Modulated Differential Scanning Calorimetry (MDSC) tests were carried out to characterise cure kinetics, glass transition temperature, and specific heat capacity of particle-filled resin samples. Laser Flash Analysis (LFA) was used to characterise the through-thickness thermal conductivity of a prepreg containing the same particle-filled resin. A finite element based analysis cure simulation model focused on heat transfer effects was developed incorporating the sub-models of cure kinetics, glass transition temperature, specific heat capacity and thermal conductivity.

2. Materials and experimental methods

2.1 Materials

The material used in this study was toughened HexPly® M21 epoxy used for primary aerospace structures [18]. The material was supplied as neat resin film containing the interleaf particles, and an epoxy prepreg with HexTow® IMA carbon fibre [19] having an areal weight of 194g/m^2 and a resin content of 34%. The matrix system, HexPly® M21 [18] is a thermoplastic interleaf particle epoxy system resulting in cured composite materials with excellent compression after impact properties appropriate for advanced aerospace applications.

2.2 Modulated Differential Scanning Calorimetry

A series of dynamic, isothermal, and cure-quenched Modulated Differential Scanning Calorimetry (MDSC) tests were performed to measure the cure kinetics, glass transition temperature evolution, and specific heat capacity of the resin. The experiments were designed using the approach outlined in [16], and the MDSC test matrix is presented in Table 1.

A TA Instruments Q2000 was used to perform the calorimetry. The instrument was calibrated prior to analysis, however the temperature and MDSC calibration was performed for each heating rate. Resin samples weighing between 6 to 8 mg were placed in the centre, flat against the bottom of aluminium hermetic Tzero™ pan. An automated sample loader was used to position the sample pan in the furnace.

The cure kinetics of the resin system was characterised using dynamic and isothermal measurements. All experiments were initially cooled to -40°C to capture the initial glass transition temperature of the material, T_{g0}. The cooling rate was set to the heating rate specified in Table 1 for the dynamic experiments, whereas the isothermal experiments were all cooled at 5°C/min to capture T_{g0}, before heating at 100°C/min to the isothermal testing temperature. Each dynamic testing condition was repeated five times and the isothermal conditions repeated three times.

The evolution of the instantaneous glass transition temperature, T_g, was captured as a function of degree-of-cure by cure-quenching select dynamic and isothermal experiments, as shown in Table 1. Cure-quenching was performed by rapidly cooling the sample to -40°C before re-scanning the sample. The cured-quenched samples were heated at 5°C/min with a modulation of ± 1.25°C per 60s to 300°C to measure the T_g evolution. Each cure-quench condition was repeated twice; some conditions returned a noticeable variation and were repeated a third time.

The resin specific heat capacity, c_{pr}, was measured by heating samples at 10°C/min to 60°C and maintaining a constant temperature for 30min before heating at 100°C/min to the testing temperatures/ times identified in Table 1. An intermediate hold at 60°C was introduced to measure the initial specific heat capacity at essentially zero degree-of-cure. Each experiment was duplicated.

2.3 Laser Flash Analysis

A Netzsch LFA 427 was used to characterise the through-thickness thermal conductivity of the IMA/M21 prepreg. Samples were mounted in a fixed volume sample holder featuring a 1.5mm thick thermoplastic ring with an 18mm internal diameter. Stainless steel disks sandwich the samples on both exterior surfaces to prevent resin flow onto the laser. The sample comprised eight layers of prepreg, laid-up in a symmetric cross-ply $[0°/90°]_{4S}$ orientation. Previous work has shown that this prepreg material consolidates under pressure at elevated temperatures [20], indicating that internal porosity is filled with resin as the viscosity softens during heating. Therefore, to minimise the potential loss in contact between the prepreg sample and the sample holder, the prepreg sample was pre-consolidated at 60°C for 30min under 700 kPa in an autoclave.

The LFA instrument was heated at 5°C/min to isothermal testing temperatures of 140, 160, 180 and 200°C. Once within 5°C of the set-point, a laser pulse was flashed on the lower side of the sample and an infrared detector measured the relative temperature increase on the opposite side of the sample [21]. A measurement was taken every 10 minutes with a signal acquisition duration of approximately 20 seconds. Each experiment was duplicated and the

sample temperature was used to calculate the degree-of-cure at each measurement using the cure kinetics model presented in section 4.1.1.

The laser flash method yields the thermal diffusivity in the through-thickness direction, which is linked to thermal properties as follows:

$$D_{th} = \frac{K_{33}}{\rho c_p} \tag{1}$$

where K_{33} and is the composite through-thickness thermal conductivity and ρ is the density of the composite. The density was calculated using the rules of mixtures by assuming a nominal fibre volume fraction, v_f of 60 %, and fibre and resin densities, ρ_f and ρ_r of 1.78g/cm^3 and 1.28g/cm^3, respectively [18,19].

$$\rho = v_f \rho_f + \left(1 - v_f\right)\rho_r \tag{2}$$

Each isothermal condition was duplicated for a total of eight experiments.

2.4 Model validation experiments

A thick laminate was cured using the manufacturer's recommended cure cycles to validate whether the heat transfer model (see section 4.1.5) developed in this study could capture the curing behaviour of IMA/M21 prepreg. The target cure cycles were developed from the Manufacturer's datasheets [18]:

- Cure cycle 1: ramp 2 °C/min to 180 °C, hold 2 h, ramp 2 °C/min to 40 °C (for laminate thickness less than 15 mm)
- Cure cycle 2: ramp 1° C/min to 150 °C, hold 3 h, ramp 1 °C/min to 180 °C, hold 2 h, ramp 2 °C/min to 40 °C (for laminate thickness greater than 15mm)

Thermocouples (K-type) were distributed through the thickness of a 130 layer IMA/M21 symmetric cross-ply laminate measuring 100 mm × 100 mm. The thickness of the cured laminate was 24.3 mm and the positions of the thermocouples are shown in Figure 1.

The laminates were cured in an autoclave at 700 kPa applied pressure and -20 kPa vacuum was maintained throughout elevated temperature processing. The laminate was placed on a 600 mm × 600 mm × 8 mm flat aluminium tool, with 50 mm silicone wide edge dams. Ultraweave 1032 breather was wrapped around the edge dams and two layers were placed on top of the laminate. A release film was placed between the laminate and the tool/ breather. The heat transfer coefficient of the autoclave at 700 kPa was measured during the two cure cycles. A 16 mm diameter, 76mm long steel rod was placed under the tool and beside the tool to measure the temperature between the air, T_A, and the centre of the rod, T_S [22]. The density of the steel rod, ρ_s, of 7707 kg/m^3 was calculated directly from the mass and volume, and a specific heat capacity, c_{ps}, of 0.49 kJ/kg/K [23], the autoclave heat transfer coefficient, HTC, was calculated using the following equation [22]:

$$HTC = \frac{\rho_s c_{ps} V \frac{dT_S}{dt}}{A(T_A - T_S)} \tag{3}$$

where A is the exposed surface area and V is the volume of the steel rod. It was shown that the heat convection coefficients on the top and bottom surfaces of this autoclave were 138 and 142 W/m^2/K, respectively.

3. Cure simulation model

A simulation of heat transfer effects occurring during the cure of IMA/M21 prepreg was developed and implemented using the commercial finite element analysis solver Abaqus/Standard. The model was three dimensional and transient. The modelling approach

used in this study was based on 3D 8- node linear heat transfer brick elements; DC3D8 Abaqus/Standard element type appropriate for heat transfer analysis. The material properties depend on both the degree-of-cure and temperature and the developed material sub-models of cure kinetics, glass transition temperature, specific heat capacity and thermal conductivity were implemented in the user defined subroutine UMATHT [24].

The cure of the 24.3 mm thick carbon fibre epoxy flat panel fabricated in an autoclave was simulated using the developed finite element based cure simulation model and the results were compared with the corresponding experimental data (Section 2.4). In the case of a flat laminate, the heat transfer problem is solved as a 1D problem with a stack of 3D elements, given that the geometry is fully symmetric in the in-plane direction. The model comprised the aluminium tool and the laminate; the breather was not taken into account since its thickness was considerably reduced during consolidation. Two case studies were investigated applying the recommended manufacturer's cure cycles as described in section 2.4. In both cases surface film condition interaction was applied at the top of the laminate and bottom of the tool representing the autoclave heat transfer coefficients. In addition, adiabatic conditions were applied at the lateral boundaries of the domain assuming no heat loss due to the high width to thickness ratio resulting in a one-dimensional thermal field.

4. Results

4.1 Thermochemical properties sub-models

4.1.1 Cure kinetics

An example of the signals obtained during a dynamic MDSC experiment is shown in Figure 2. The advantage of the MDSC over conventional DSC is that the total heat flow signal can be separated into the non-reversible and reversible signals. In the case of thermoplastic particle interleaf systems the advantage of splitting the heat flow signals is that the non-reversible signals captures the energy released during the cross-linking reaction and the

reversible signal is more sensitive to phase changes, such as rubbery to glassy transitions and melting. The blip observed on the total heat flow signal just above 195°C in Figure 2 is accentuated in the reversible signal. The endothermic event could reflect a melting phase-change of the interleaf particles.

The degree-of-cure, α, at any time τ, can be evaluated using the following expression [9]:

$$\alpha(\tau) = \frac{\int_{t_1}^{\tau} \frac{dH(t)}{dt} dt}{H_T} \tag{4}$$

Here t_1 is the time the reaction started, whilst $H(t)$ is the heat released at any time t, and H_T is the total heat of reaction. The total heat of reaction H_T is calculated by integrating the total area enclosed by the thermogram during dynamic cure.

$$H_T = \int_{t_1}^{t_2} \frac{dH}{dt} dt \tag{5}$$

Here t_2 denotes the time the reaction completed.

In the case of dynamic cure, the resin absorbs or emits heat, at a rate depending on its heat capacity evolution. Therefore, an appropriate baseline should be chosen being able to reflect this phenomenon in order to carry out the integration shown in Eqns. (4) and (5). A linear or sigmoidal baseline is often used to integrate the heat flow signal, however, there is no experimental evidence that the material emits or absorbs heat in a sigmoidal or linear fashion. Therefore, an iterative baseline [25, 26] was chosen to perform the integration of heat flow versus time as presented in Eqns. (4) and (5). This yielded a mean value in total heat of reaction value of 415 J/g with a coefficient of variation of 2.8%, implying that the effect of heating rate is negligible on the total heat of reaction. In the case of isothermal scans, a

horizontal baseline was implemented, whilst the mean value of the total heat of reaction calculated during the dynamic scans was used to perform the integration described by Eq. (4).

The modelling methodology adopted here was first to develop a cure kinetics model in the case of isothermal cure leading to a first approximation of the kinetic parameters. This model was then fitted to the dynamic scans for an accurate estimation of the cure kinetics parameters. The model applied to the isothermal cure was an autocatalytic model described by the following equation [9]:

$$\frac{d\alpha}{dt} = (k_1 + k_2\alpha^m)(1-\alpha)^n \tag{6}$$

Here $\frac{d\alpha}{dt}$ is the cure reaction rate, m and n are reaction orders, and k_1, k_2 are reaction rate constants following an Arrhenius temperature dependence:

$$k_i = A_i e^{\left(\frac{-E_i}{RT}\right)}, i = 1,2 \tag{7}$$

where T is the current temperature, E_1, E_2 are activation energies, and A_1, A_2 are pre-exponential Arrhenius constants. A first approximation of k_1 was determined using the initial reaction rate values as proposed in [27], whereas the remaining parameters of Eq. (6) were estimated using Eq. (8) [9]. In specific, the isothermal scans were used to plot the left hand side of Eq. (8) versus $ln\alpha$, which yields a straight line with intercept $\ln k_2$ and slope m [9]:

$$\ln\left(\frac{\frac{d\alpha}{dt}}{(1-\alpha)^n} - k_1\right) = \ln k_2 + m\, ln\alpha \tag{8}$$

The cure kinetics model developed using solely the isothermal scans presented a poor fit to the dynamic cure response; this was most likely due to the narrow temperature range for

which the model parameters were evaluated. To capture the cure behaviour more accurately Eq. (5) was modified to [9]:

$$\frac{d\alpha}{dt} = k_1(1-\alpha)^{n_1} + k_2\alpha^m(1-\alpha)^{n_2} \tag{9}$$

The cure kinetics model described by Eq. (9) was fitted to the dynamic runs using the generalised reduced gradient non-linear optimization method implemented in Microsoft Excel [28]. To further improve the accuracy of the model diffusion rate limitation phenomena were incorporated by introducing a diffusion term in the reaction rate constants (see Eq. (7)) as follows [29]:

$$\frac{1}{k_i} = \frac{1}{k_{iC}} + \frac{1}{k_D} \quad i = 1,2 \tag{10}$$

here k_{iC} are the chemical rate constants following an Arrhenius temperature dependence:

$$k_{iC} = A_i e^{\left(\frac{-E_i}{RT}\right)} \quad i = 1,2 \tag{11}$$

and k_D is a diffusion rate constant defined as follows:

$$k_D = A_D e^{\left(\frac{-E_D}{RT}\right)} \tag{12}$$

where A_D and E_D denote the pre-exponential factor and activation energy associated with the diffusion rate limitation phenomena, respectively, b a constant, and f the equilibrium free volume defined as:

$$f = w\left(T - T_g\right) + g \tag{13}$$

here w and g are constants and T_g is the instantaneous glass transition temperature (see section 4.1.2).

The diffusion terms presented in Eqns. (10)- (13) were estimated by fitting the cure kinetics model to the isothermal scans using the generalised reduced gradient non-linear optimization

method implemented in Microsoft Excel [28]. Table 2 summarises the cure kinetics parameters identified using this modelling methodology.

Figure 3 and Figure 4 show that the developed cure kinetics model is in quite good agreement with the experimental behaviour in both dynamic and isothermal conditions, implying that the developed cure kinetics models is able to predict the cure behaviour of the epoxy system considered in this study accurately. One drawback of this model is that it struggles to capture any phase-change events that take place during heating; Figure 3 shows a wobble in the cure rate signal when the endothermic event (see Figure 2) was observed. This is not captured by the current cure kinetics model, and to the best of our knowledge, there are currently no phenomenological models able to capture this behaviour.

The isothermal measurements presented in Figure 4 show that the cure kinetics model is capable of capturing the peak in cure rate at a degree-of-cure of approximately 0.1 to 0.15, followed by a linear decreasing cure rate as the degree-of-cure advances. A higher dispersion between experimental repeats was observed with increasing temperature. This dispersion is a drawback of isothermal DSC testing, where both the instrument and sample have less time to equilibrate with the desired dwell temperature. As a result, cure reaction information is lost at low levels of conversion, as observed above 190°C, where the peak in cure rate of the model and is slightly off-set.

4.1.2 Glass transition temperature

The evolution of T_g as a function of the degree-of-cure for both the isothermal and dynamic runs is presented in Figure 5. A unique T_g- α relationship was observed and the DiBenedetto [30] equation was used to model the evolution of the glass transition temperature as follows:

$$\frac{T_g - T_{g0}}{T_{g\infty} - T_{g0}} = \frac{\lambda\alpha}{1-(1-\lambda)\alpha} \quad (14)$$

where T_{g0} is the uncured glass transition temperature of 1.5 °C, $T_{g\infty}$ is the ultimate glass transition temperature of 194°C, α is the instantaneous degree-of-cure, and λ is a fitting parameter governing the convexity of the curve that was found to best approximate the experimental data at a value of 0.67 using the generalised reduced gradient non-linear optimization method [28].

4.1.3 Specific heat capacity

Figure 6 depicts the specific heat capacity of the resin in the temperature- degree-of-cure space during the different isothermal runs. The step change presented here indicates the transition from the rubbery to the glassy state (glass transition) of the thermosetting material. The resin specific heat capacity depends on both the degree-of-cure and temperature. In particular, there is a linear dependence on temperature, whilst the dependence on degree-of-cure can be expressed as a transition around the instantaneous glass transition temperature (Eqn. (14)) as follows [31]:

$$c_{pr} = A_{rc_p}T + B_{rc_p} + \frac{\Delta_{rc_p}}{1 + e^{C_{rc_p}(T - T_g - s)}} \quad (15)$$

Here A_{rc_p} and B_{rc_p} are constants expressing the linear dependence of the resin specific heat capacity on temperature for constant material state, while Δ_{rc_p} , C_{rc_p} and s are constants referring to the strength, breadth and temperature shift of the transition around the T_g. The values of the specific heat capacity coefficients were estimated by fitting Eq. (15) to the experimental data shown in Figure 6 using the generalised reduced gradient non-linear optimization method and are reported in Table 3. There is a quite good agreement between

the model and the experimental data with the model being able to capture accurately the transition from the rubbery to the glassy state of the material due to vitrification. Note that in the case of 200°C no transition is present, implying that the material remains in the rubbery state. This is due to the fact that the cure temperature in this case (200°C) is considerably higher than the ultimate T_g throughout the whole cycle so that no vitrification occurs.

The specific heat capacity of the fibre can be expressed as linear function of temperature as follows [22]:

$$c_{pf} = A_{fc_p} T + B_{fc_p} \tag{16}$$

where A_{fc_p} is 0.00205 [1/g/°C^2] and B_{fc_p} is 0.75 [1/g/°C].

The specific heat capacity of the composite is computed using the rule of mixtures:

$$c_p = w_f c_{pf} + \left(1 - w_f\right) c_{pr} \tag{17}$$

Here w_f is the fibre weight fraction and is defined as

$$w_f = \frac{v_f \rho_f}{\rho} \tag{18}$$

4.1.4 Thermal conductivity

Figure 7 depicts the through- thickness thermal conductivity of IMA/M21 prepreg for the different experimental runs. The thermal conductivity increases with the degree-of-cure, whilst for a given degree-of-cure it decreases with temperature as shown in Figure 7. Multivariate regression was carried out on the experimental data shown in Figure 7 and the following model has been used for the through- thickness thermal conductivity of IMA/M21 prepreg:

$$K_{33} = A_{kr}T\alpha + B_{kr}\alpha + C_{kr}T + D_{kr} \quad (19)$$

The thermal conductivity parameters presented in Eq. (19) are summarised in Table 4.

4.1.5 Model validation

Figures 8 and 9 depict the temperature evolution at different positions through the thickness for the two cure cycles, respectively. There is excellent agreement between the cure simulation results and the experimental data for both cases implying that the developed heat transfer model is capable of predicting the cure behaviour of IMA/M21 prepreg accurately. As Figure 8 shows the temperature of the laminate is initially lower than the autoclave temperature, whereas a temperature overshoot occurs at the beginning of the first dwell due to the exothermic reaction. This is followed by a decrease until the end of the cycle. This is attributed to the high temperature gradients, caused by the low through thickness thermal conductivity of the material. These phenomena are more pronounced between 12mm and 18mm presenting a temperature overshoot in the order of 14.2 and 14.5°C, respectively, whilst the temperature overshoot at 6mm is around 9.2°C. Similarly, in the case of Cure Cycle 2 (Figure 9) a temperature overshoot is presented at the beginning of the first dwell, however, it is low ranging from 5 to 6°C.

A micrograph of a cured IMA/M21 laminate is shown in Figure 10, revealing distinct resin rich regions with particles between the fibre reinforcement layers. The overall composite is considered homogeneous in the numerical model. The simulation predictions agree with the experimental data (see Figures 8 and 9), indicating that the homogeneity assumption is correct in terms of heat transfer effects at the lamina level as potential temperature differences within a layer of prepreg at the particle level is insensitive to the heat transfer mechanisms. This is reinforced by the fact that the properties and reaction rates measured during the material characterisation result in appropriate representation of the global laminate

heat transfer effects by the model. If the scale of homogenisation did not match the scale of the heat transfer effects, significant discrepancies between the model response and the experimental data shown in Figures 8 and 9 would appear.

4.1.6 Sensitivity analysis

A sensitivity analysis was carried out using Cure cycle 1 (see section 2.4) to investigate the effect of ramp rate, cure temperature and laminate thickness on temperature overshoot and cure time. Three ramp rates of 1, 2 and 4°C/min were investigated. The cure temperature was varied between 160 to 200°C using an interval of 10°C. Three laminate thicknesses of 15, 24 and 35 mm were studied. In this study, cure time is considered the time at which the minimum degree-of-cure of the laminate is higher or equal than 0.9.

Figures 11 and 12 summarise the sensitivity analysis results. There is a clear trade- off between temperature overshoot and cure time highlighting the competitive nature between these two parameters. Increasing the ramp rate reduces the cure time and increases the temperature overshoot due to higher reaction rates. As expected, increasing the laminate thickness results in higher temperature overshoots due to low thermal conductivity in the through the thickness direction. Nevertheless, laminate thickness has a negligible effect on cure time (Figure 11 (b)). This is attributed to the fact that in all case studies both the bottom and top surfaces of the manufactured part are the last to cure given that there is an overshoot for all studied thicknesses. The results shown in Figure 12 can be clustered in two regions; a region where cure time is minimised and temperature overshoot can be significantly reduced with small changes in cure time and a region of high cure times where significant improvements in cure time can be achieved with small changes in temperature overshoot. This underlines the competitive nature of cure time and temperature overshoot. It is noteworthy that these regions do not always correspond to similar process parameters, i.e.

neighbouring point in the process outcome space may correspond to different process parameters. The region of low temperature overshoots and high cure times correspond to the manufacturer's recommended cure cycle 1 (see section 2.4) pointing out the conservative nature of current process designs implying that the manufacturer's recommended cure cycle can lead to prolonged process cycles with significant cost implications. As Figures 11 and 12 show, a decrease in cure time in the order of 22.5–23% can be achieved with a corresponding increase in temperature overshoot between 5–12.5% by using a ramp rate of 4°C/min instead of 2°C/min and a cure temperature of 180°C demonstrating the potential for significant efficiency improvements in process design. In addition, the results presented here provide valuable information around process design in terms of laminate thickness.

5. Conclusions

The cure behaviour of a particle interleaf carbon fibre epoxy prepreg system was successfully characterised and modelled using methodologies typically applied to non-particle interleaf systems. A cure simulation model focusing on the heat transfer effects was developed including sub-models of cure kinetics, glass transition temperature, specific heat capacity and thermal conductivity. Through experimental validation it was shown that the developed model is appropriate for simulating the cure process of thermoplastic particle interleaf carbon fibre epoxy prepregs accurately. The cure simulation model was applied successfully to inform the process design space for different laminate thicknesses in a sensitivity analysis. The results highlighted the conservative nature of the conventional process cycles, and outlined opportunities to increase efficiency and productivity during manufacture. Further development of simulation capabilities to introduce the development of residual stresses and integrate cure simulation with consolidation models for this class of materials will lead to predictive capabilities for the full process chain and the ability to investigate, design and optimise the manufacturing of interleaf carbon fibre epoxy prepreg components.

Data Access Statement

The experimental data is available for download from the Research Data Repository of University of Bristol at https://data.bris.ac.uk/data/dataset/3utcijc5qldfl2j70blaey80vo

Acknowledgements

This work was supported by the Engineering and Physical Sciences Research Council [grant number EP/1033513/1], through the EPSRC Centre for Innovative Manufacturing in Composites (CIMComp) project “Defect Generation Mechanisms in Thick and Variable Thickness Composite Parts”. The materials used in this project were kindly donated by Hexcel.

References

[1] Hojo M, Matsuda S, Tanaka M, Ochiai S, Murakami A. Mode I delamination fatigue properties of interlayer-toughened CF/epoxy laminates. Composites Science and Technology. 2006 May 31;66(5):665-75.[2] [2] Hodgkin, J.H., Simon, G.P. and Varley, R.J., 1998. Thermoplastic toughening of epoxy resins: a critical review. Polymers for Advanced Technologies, 9(1), pp.3-10.

[3] Stevanovic D, Kalyanasundaram S, Lowe A, Jar PYB. Mode I and mode II delamination properties of glass/vinyl-ester composite toughened by particulate modified interlayers. Compos Sci Technol 2003;63:1949–64.

[4] Singh S, Partridge IK. Mixed-mode fracture in an interleaved carbon-fibre/epoxy composite. Compos Sci Technol 1995;55(4):319–27.

[5] Partridge I, Cartié D. Suppression of initiation of delamination cracking in unidirectional composites by self-same resin interleaving. Appl Fract Mech Polym, Adhésives Compos 2004:33.

[6] Bogetti TA, Gillespie JW. Process-Induced Stress and Deformation in Thick-Section Thermoset Composite Laminates. Journal of Composite Materials. 1992;26(5):626-60.

[7] Cavarero M, Olivier P, Cottu JP. Computer-aided design and manufacture: software for the definition of the curing conditions of composite material parts. Computer Aided Design in Composite Material Technology - International Conference. 1996. p. 297-306.

[8] Sourour S, Kamal MR. Differential scanning calorimetry of epoxy cure: isothermal cure kinetics. Thermochimica Acta. 1976;14(1–2):41-59.

[9] Karkanas PI, Partridge IK. Cure modeling and monitoring of epoxy/amine resin systems. I. Cure kinetics modeling. J Appl Polym Sci 2000;77(7):1419-1431.

[10] Lee JY, Choi HK, Shim MJ, Kim SW. Kinetic studies of an epoxy cure reaction by isothermal DSC analysis. Thermochimica Acta. 2000;343(1–2):111-7.

[11] Pascault JP, Williams RJJ. Formulation and characterization of thermoset-thermoplastic blends. In: Paul DR, Bucknall CB, editors. Polymer Blends. New York: John Wiley and Sons, Inc.; 2000. p. 379-41.

[12] Williams RJ, Rozenberg BA, Pascault J-P. Reaction-induced phase separation in modified thermosetting polymers. Polymer Analysis Polymer Physics: Springer; 1997. p. 95-156.

[13] Zhang J, Fox BL. Manufacturing influence on the delamination fracture behavior of the T800H/3900-2 carbon fiber reinforced polymer composites. Mater Manuf Process 2007;22:768–72.

[14] Abou Msallem Y, Jacquemin F, Boyard N, Poitou A, Delaunay D, Chatel S. Material characterization and residual stresses simulation during the manufacturing process of epoxy matrix composites. Composites Part A: Applied Science and Manufacturing. 2010;41(1):108-15.

[15] Paris C, Bernhart G, Olivier PA, De Almeida O. Influence de cycles de cuisson rapides sur le preimpregne aeronautique M21/T700: suivi de polymerisation et proprietes mecaniques. Materiaux et Techniques. 2012;100(6-7):611-22.

[16] Dykeman D. Minimizing uncertainty in cure modeling for composites manufacturing. PhD Thesis, The University of British Columbia, Vancouver, 2008.

[17] Paris C. Étude et modélisation de la polymérisation dynamique de composites à matrice thermodurcissable PhD thesis. INP Toulouse; 2011.

[18] Hexcel Composites SA, HexPly® M21 product data sheet. www.hexcel.com, 2010.

[19] Hexcel Composites SA, HexTow® IMA Carbon Fibre Product Data Sheet. www.hexcel.com, 2016.

[20] Belnoue JPH, Nixon-Pearson OJ, Ivanov D, Hallett SR. A novel hyper-viscoelastic model for consolidation of toughened prepregs under processing conditions. Mechanics of Materials. 2016;97:118-34.

[21] Laser Flash Analysis – LFA Method, Technique, Applications. https://www.netzsch.com/en/, 2016.

[22] Johnston A. An integrated model of the development of process-induced deformation in autoclave processing of composite structures, PhD Thesis, University of British Columbia, 1997.

[23] Ashby M, Shercliff H, Cebon D. Materials: Engineering, Science, Processing and Design. Elsevier, 2007.

[24] Abaqus 6.14 Documentation. http://abaqus.software.polimi.it/v6.14/index.html, 2015.

[25] Bandara U. (1986), A systematic solution to the problem of sample background correction in DSC curves, Journal of Thermal Analysis and Calorimetry, vol. 31, no. 5, pp. 1063-1071.

[26] Skordos A, Partridge I. Cure kinetics modeling of epoxy resins using a non-parametric numerical procedure. Polymer Engineering & Science 2001;41(5):793-805.

[27] Ryan, M.E. and Dutta, A., 1979. Kinetics of epoxy cure: a rapid technique for kinetic parameter estimation. Polymer, 20(2), pp.203-206.

[28] Press WH. Numerical recipes 3rd edition: The art of scientific computing. Cambridge university press, 2007.

[29] Karkanas PI, Partridge IK, Attwood D. Modelling the cure of a commercial epoxy resin for applications in resin transfer moulding. Polymer International. 1996 Oct 1;41(2):183-91.

[30] DiBenedetto A. Prediction of the glass transition temperature of polymers: a model based on the principle of corresponding states. Journal of Polymer Science Part B: Polymer Physics. 1987;25(9):1949-69.

[31] Mesogitis, T.S., Skordos, A.A. and Long, A.C., 2015. Stochastic simulation of the influence of cure kinetics uncertainty on composites cure. Composites Science and Technology, 110, pp.145-151.

Table 1. MDSC Test Matrix.

	Modulation [±°C per 60s]	End temperature [°C]	Hold time [min]
Dynamic heating rate [°C/min]			
1	0.25	275	
2	0.5	150, 175, 185, 195, 200, 210, 225, 280	
5	1.25	150, 175, 185, 190, 200, 210, 225, 235, 250, 300	
10	2.5	350	
Isothermal temperature [°C]			
140	1		600
150	1		15, 30, 60, 90, 120, 150, 200, 500
160	1		400
170	1		300
180	1		7.5, 15, 30, 60, 90, 300
190	1		200
200	1		200
Specific heat capacity tests			
140	1		600
160	1		400
180	1		300
200	1		200

Table 2. Cure kinetics model parameters.

Kinetic parameter	Value
A_1	420615 [1/s]
E_1	78890 [J/mol]
A_2	57440 [1/s]
E_2	68978 [J/mol]
A_D	2.6E+20 [1/s]
E_D	87455.74 [J/mol]
m	0.6
n_1	0.8
n_2	3.2
b	1.98
w	0.000165
g	0.058235

Table 3. Resin specific heat capacity model parameters.

Parameter	Value
A_{rc_p}	0.0029 [J/g/^{0}C]
B_{rc_p}	1.84 [J/g/^{0}C]
C_{rc_p}	0.15 [J/^{0}C]
Δ_{rc_p}	-0.26 [J/g/^{0}C]
s	0.65 [^{0}C]

Table 4. IMA/M21 through thickness thermal conductivity model parameters.

Parameter	Value
A_{kr}	-1.5×10^{-3} [W/m/°C^2]
B_{kr}	0.392 [W/m/°C]
C_{kr}	-1×10^{-3} [W/m/°C^2]
D_{kr}	0.734 [W/m/°C]

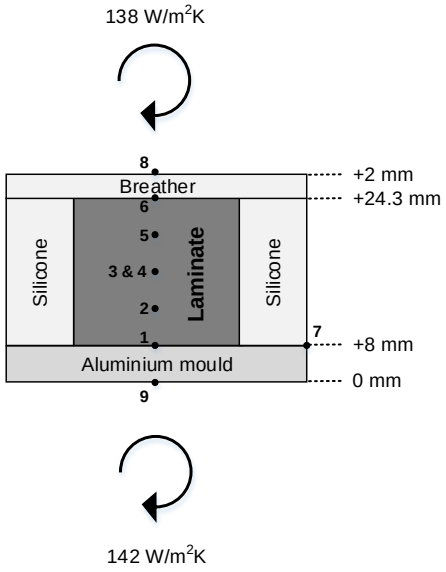

Figure 1. Experimental set-up of the thick laminate manufacture in the autoclave (left) and a schematic of the thermocouple measurements (right).

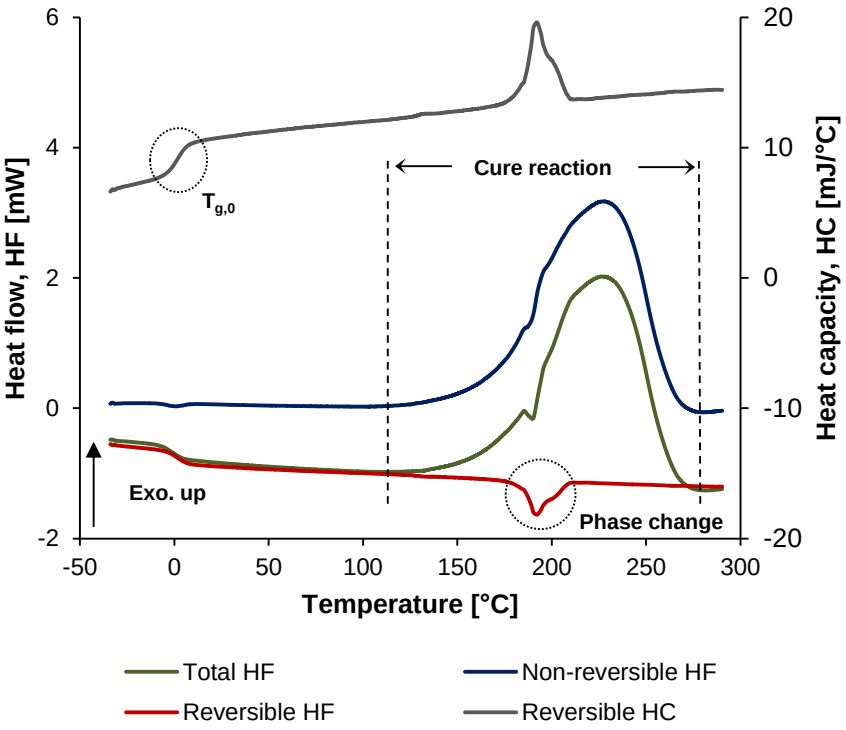

Figure 2. MDSC measurements of M21 resin during dynamic heating at 5°C/min.

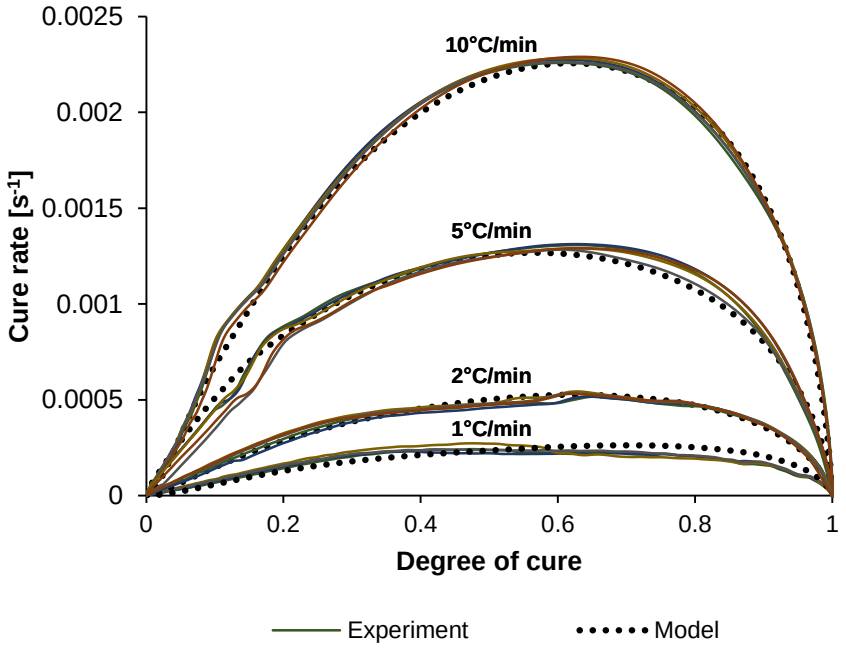

Figure 3. Dynamic cure of M21 epoxy resin.

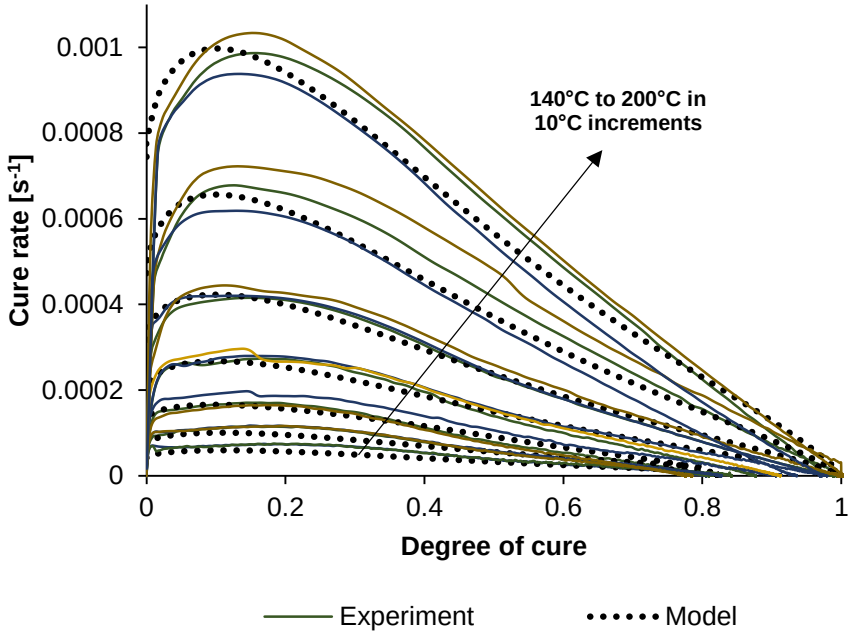

Figure 4. Isothermal cure of M21 epoxy resin.

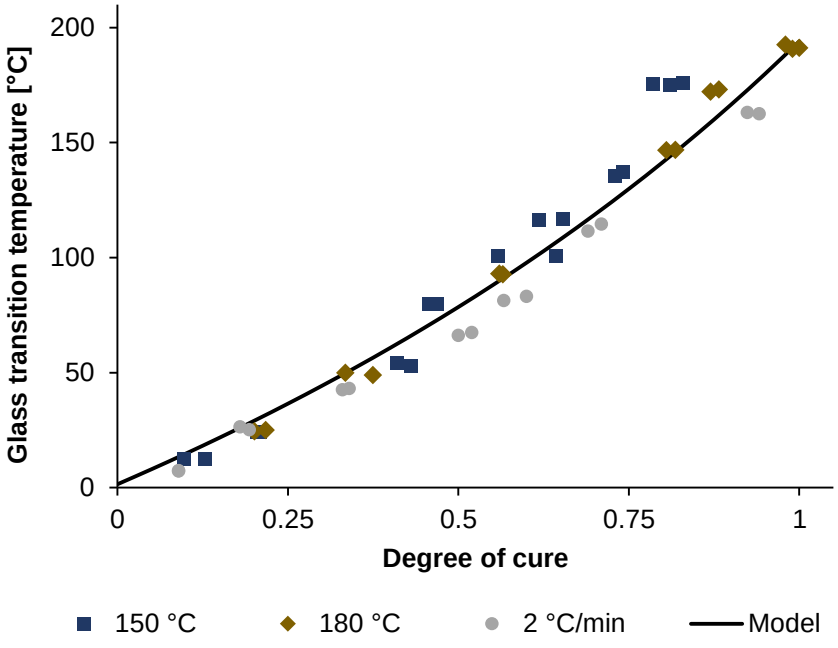

Figure 5. Glass transition temperature development of M21 obtained by cure-quenching experiments.

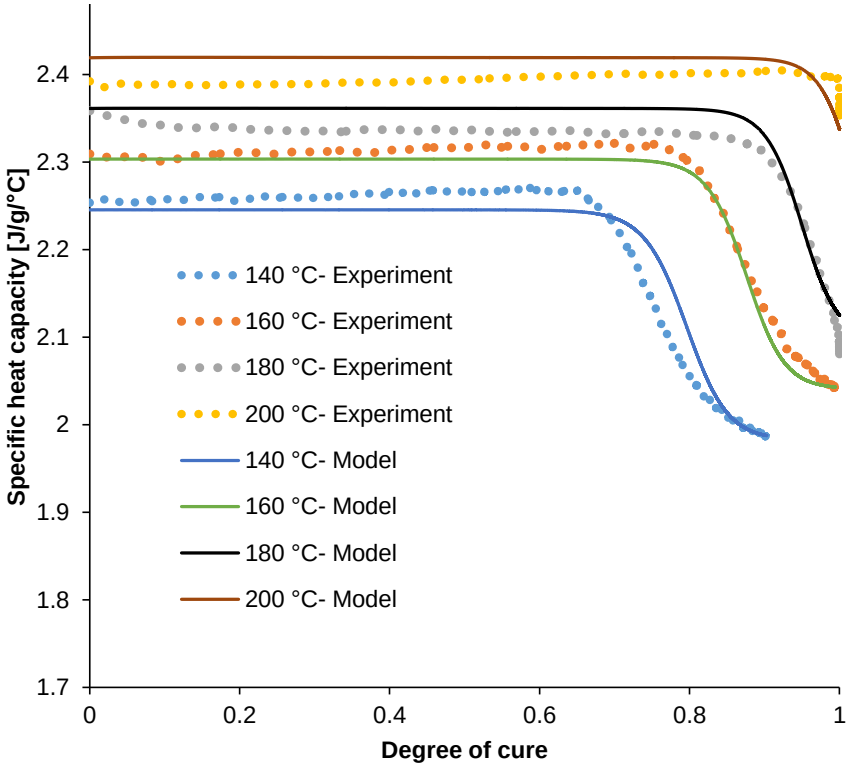

Figure 6. Specific heat capacity evolution of M21 epoxy resin.

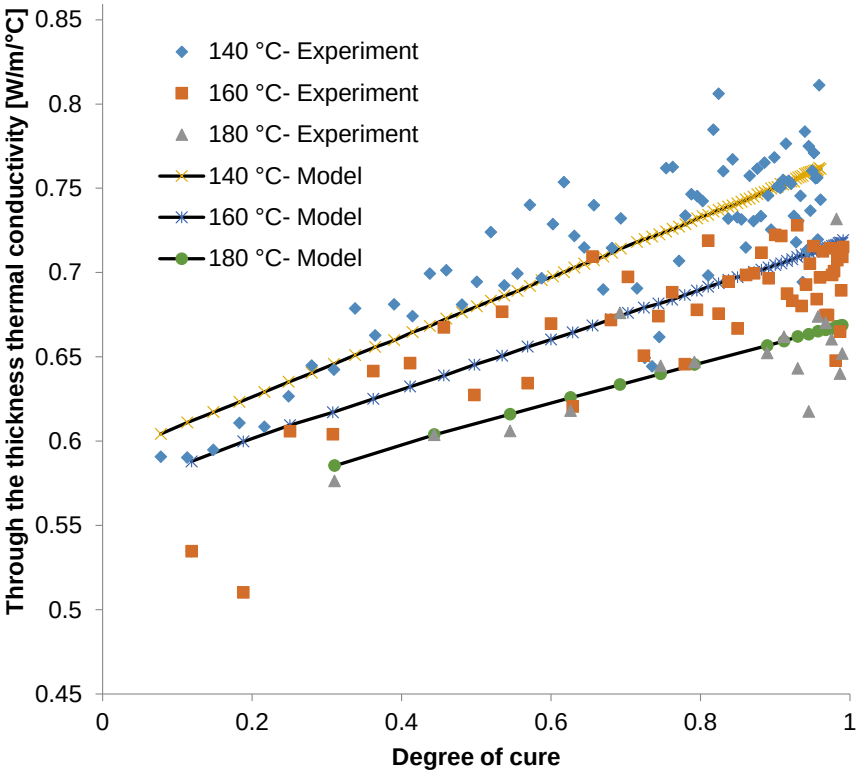

Figure 7. Through the thickness thermal conductivity evolution of IMA/M21 prepreg.

a

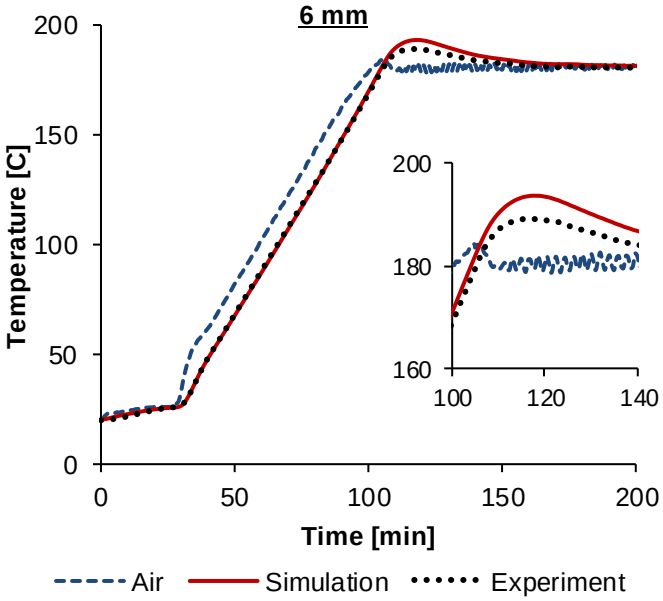

b

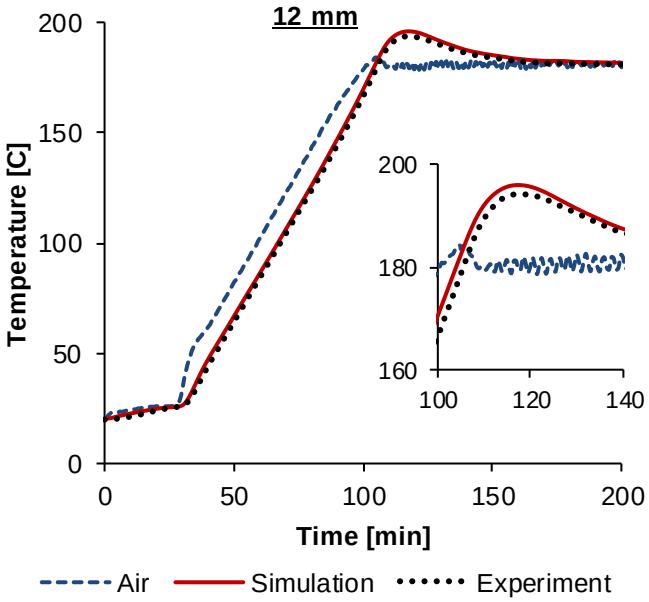

c

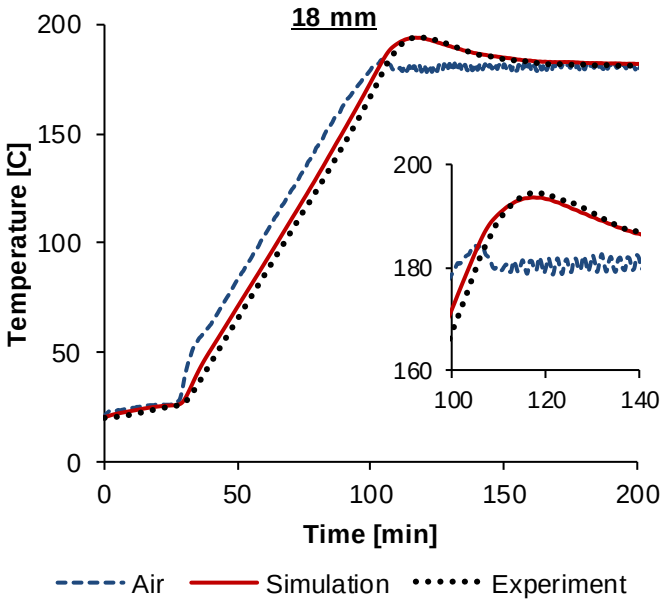

Figure 8. Cure cycle 1: simulated and measured temperature evolution in the thick composite sample. Insert shows exotherm generated at the beginning of the 180°C cure.

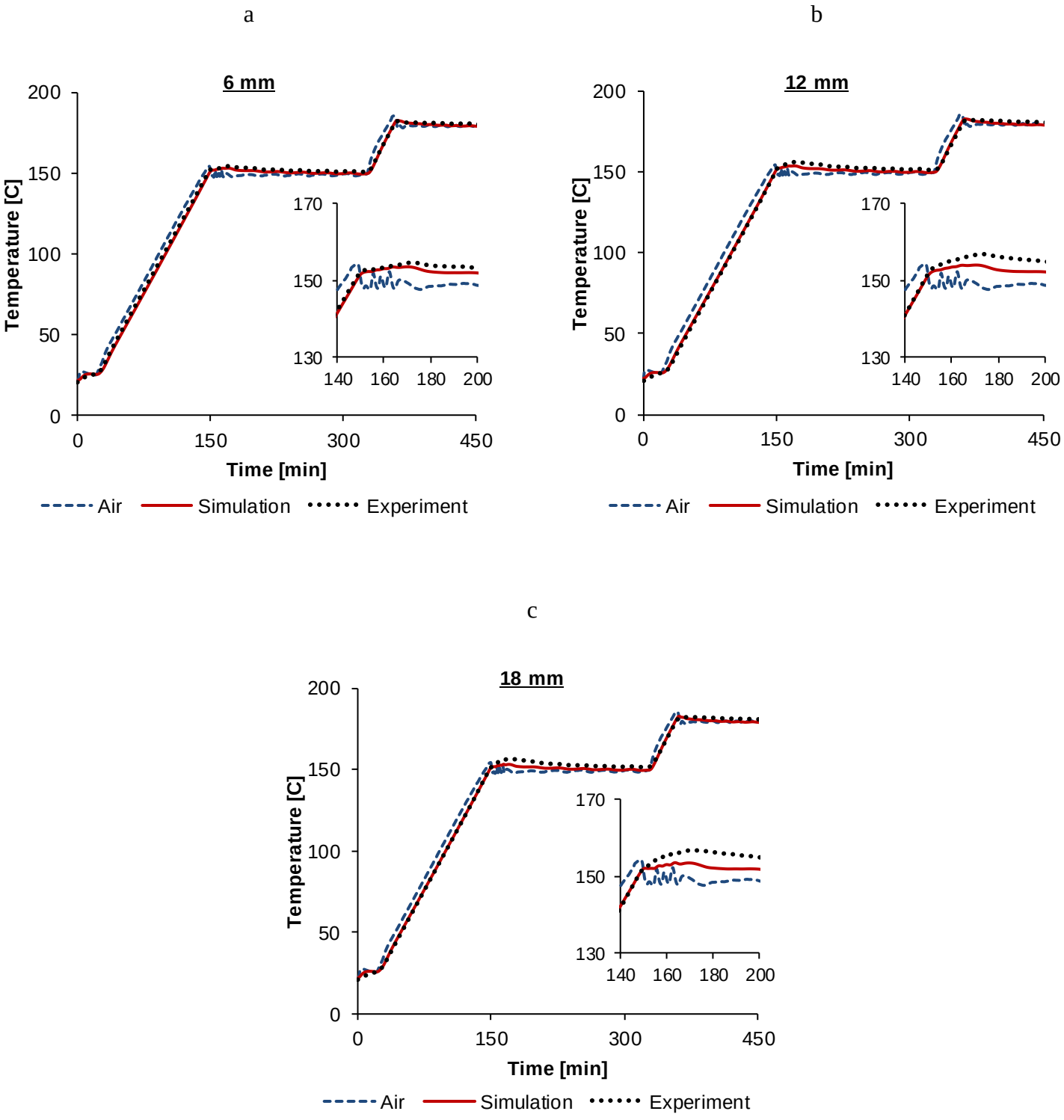

Figure 9. Cure cycle 2: simulated and measured temperature evolution in the thick composite sample. Insert shows a small exotherm at the beginning of the 150°C dwell.

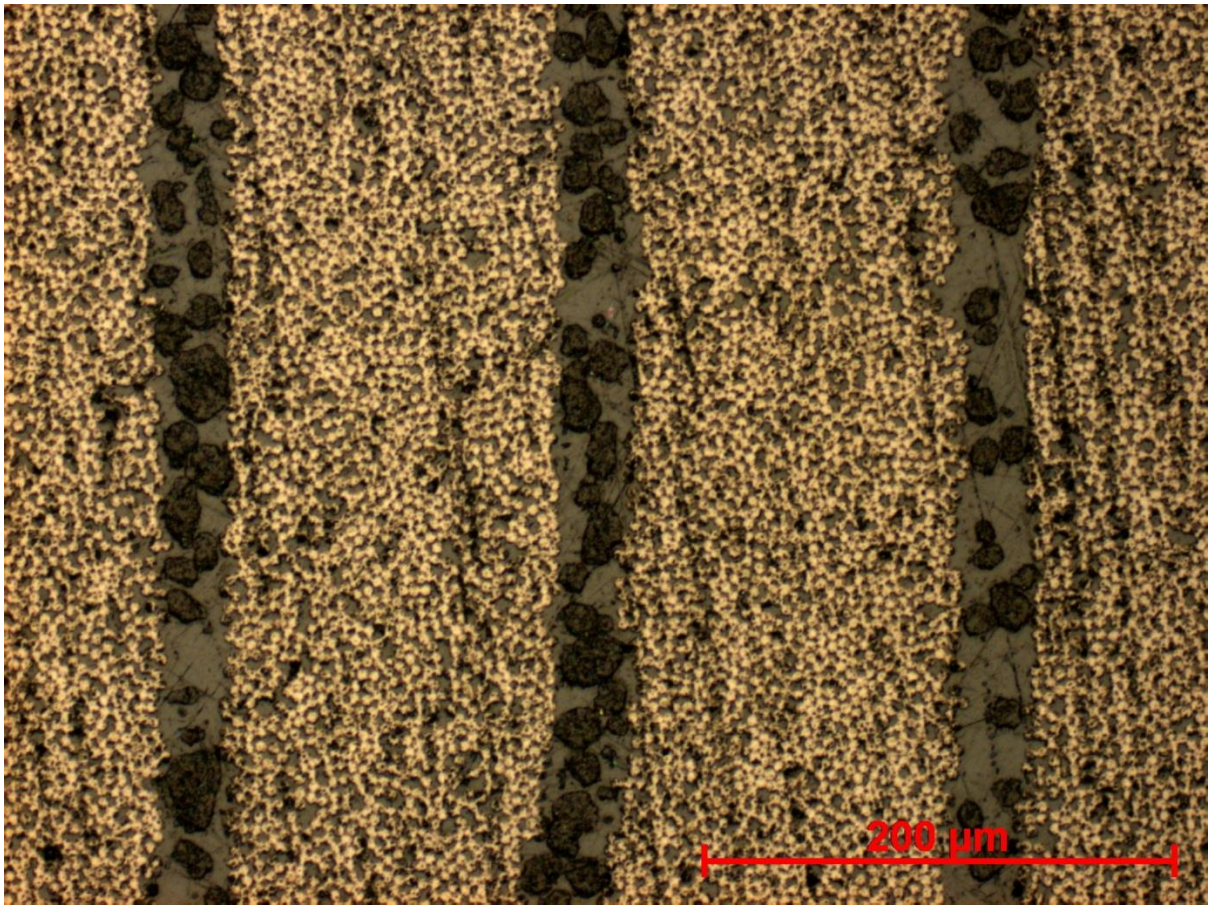

Figure 10. Micrograph of cure IMA/M21 composite.

a

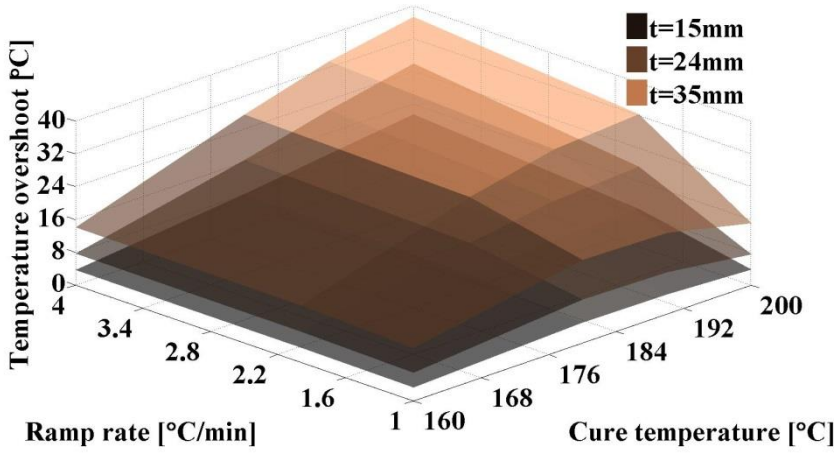

b

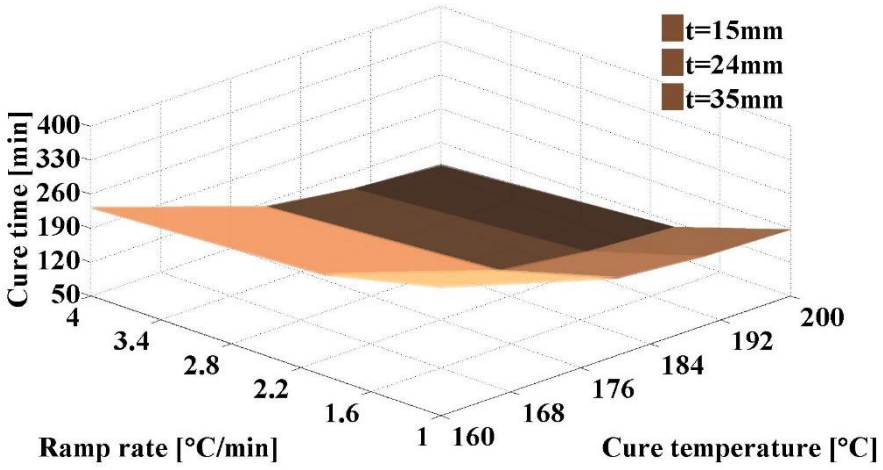

Figure 11. Sensitivity analysis results (a) temperature overshoot (b) cure time.

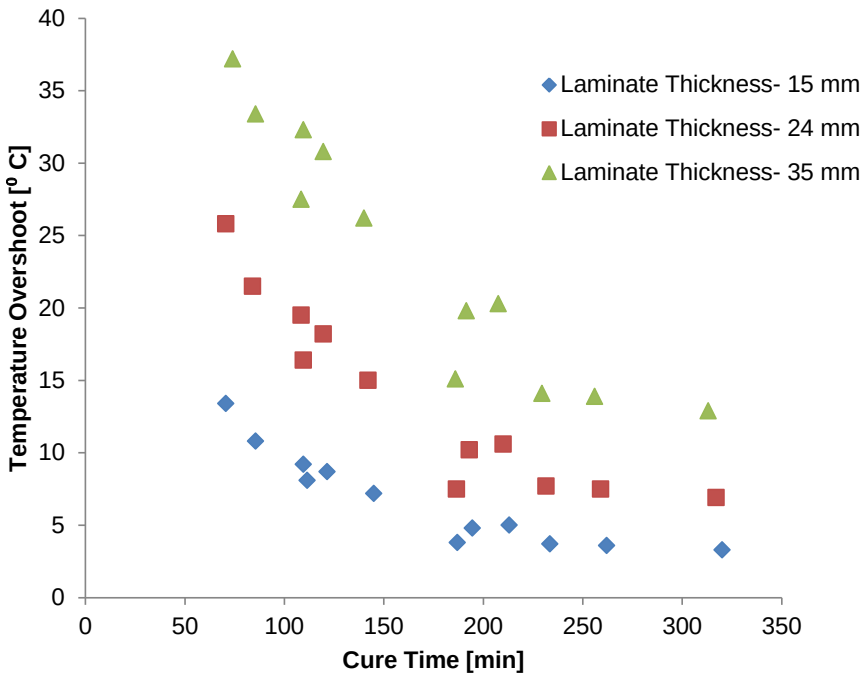

Figure 12. Sensitivity analysis results; Cure time- temperature overshoot trade-off.